Crystalline Solids of Alloy Clusters

N. Sandhyarani and T. Pradeep*

*Department of Chemistry and Regional Sophisticated Instrumentation Centre,
Indian Institute of Technology, Madras 600 036, India*

Received October 8, 1999. Revised Manuscript Received March 3, 2000

AuAg alloy clusters protected with octadecanethiol (ODT) monolayers form crystalline solids whose powder X-ray diffractograms can be indexed to single cubic unit cells. These solids can also be regarded as superlattices of alloy clusters. The bulk Au:Ag ratio is significantly different from the metal salt feed ratio used for the synthesis of the alloy clusters. The surface plasmon resonance band of the alloy clusters shift monotonically with change in composition and only one distinct band is seen in the composition range, indicating that the single metal core containing alloy clusters are not forming. The shifts observed can be linearly related to the compositions. Atomic emission spectroscopy gives similar compositions as determined from absorption spectroscopy. The monolayer coverage determined from thermogravimetry increases with an increase in silver concentration. Thermal stability of the monolayers is comparable to pure Au and Ag clusters and no change in desorption temperature is observed with composition. Both monolayer melting and superstructure melting transitions are seen in the differential scanning calorimetry of the solids. Infrared spectroscopy suggests that the monolayers are essentially solidlike and the conformations are similar to the monolayers on pure Ag clusters. Some of the bands exhibit factor group splitting in the Au-rich composition, which is observed in other compositions upon annealing.

Introduction

Monolayer-protected clusters (MPCs) are a class of molecular materials having well-defined properties, which are tunable depending on the metal, the cluster dimension, and the nature of the molecule chosen to form the monolayer.[1] A number of synthetic approaches have been suggested to prepare them, focusing on the variety of cluster dimensions achievable.[2] Studies have been made on the spectroscopy and chemistry of mono-

layers assembled on cluster surfaces;[3] most of these reports pertain to alkanethiol protected gold clusters. The monolayers of adjacent clusters interact leading to single-phase superlattices.[4] In solution, the alkyl chain ends have significant mobility due to the high curvature of the cluster surface.[4h] The solids, however, show increased order in the alkyl chain body.[4h] The interpenetration of the extended alkyl chain assembly is suggested to be the reason for superlattice formation.[4j] The X-ray diffraction data[4f] as well as energy filtered transmission electron micrographs[4j] have been interpreted in this fashion. Bundling of alkyl chains on the

* Author for correspondence. E-mail: pradeep@acer.iitm.ernet.in. Fax: ++91-44-235 0509 or 2545.

(1) (a) See for a review, Hostetler, M. J.; Murray, R. W. *Current Opin. Coll. Inter. Sci.* **1997**, *2*, 42−50. (b) Terril, R. H.; Postlethwaite, T. A.; Chen, C.-H.; Poon, C.-D.; Terzis, A.; Chen, A.; Hutchison, J. E.; Clark, M. R.; Wignall, G.; Londono, J. D.; Superfine, R.; Falvo, M.; Johnson, C. S., Jr.; Samulski, E. T.; Murray, R. W. *J. Am. Chem. Soc.* **1995**, *117*, 12537−12548. (c) Brust, M.; Fink, J.; Bethell, D.; Schiffrin, D. J.; Kiely, C. *J. Chem. Soc., Chem. Commun.* **1995**, 1655−1656. (d) Leff, D. V.; Brandt, L.; Heath, J. R. *Langmuir* **1996**, *12*, 4723−4730. (e) Leff, D. V.; Ohara, P. C.; Heath, J. R.; Gelbart, W. M. *J. Phys. Chem.* **1995**, *99*, 7036−7041. (f) Alvarez, M. M.; Khoury, J. T.; Schaaff, T. G.; Shafigullin, M. N.; Vezmar, I.; Whetten, R. L. *J. Phys. Chem. B* **1997**, *101*, 3706−3712. (g) Vijaya Sarathy, K.; Raina, G.; Yadav, R. T.; Kulkarni, G. U.; Rao, C. N. R. *J. Phys. Chem. B* **1997**, *101*, 9876− 9880. (h) Chen, S.; Murray, R. W. *Langmuir* **1999**, *15*, 682−689. (i) Crooks, R. M.; Zhao, M. *Adv. Mater.* **1999**, *11*, 217−220.

(2) (a) Brust, M.; Walker, M.; Bethell, D.; Schiffrin, D. J.; Whyman, R. *J. Chem. Soc., Chem. Commun.* **1994**, 801−802. (b) Johnson, S. R.; Evans, S. D.; Mahon, S. W.; Ulman, A. *Langmuir* **1997**, *13*, 51−57. (c) Hostetler, M. J.; Wingate, J. E.; Zhong, C.-J.; Harris, J. E.; Vachet, R. W.; Clark, M. R.; Londono, J. D.; Green, S. J.; Stokes, J. J.; Wignall, G. D.; Glish, G. L.; Porter, M. D.; Evans. N. D.; Murray, R. W. *Langmuir* **1998**, *14*, 17−30. (d) Vijaya Sarathy, K.; Kulkarni, G. U.; Rao, C. N. R. *J. Chem. Soc., Chem. Commun.* **1997**, 537−538. (e) Garcia, M. E.; Baker, L. A.; Crooks, R. M. *Anal. Chem.* **1999**, *71*, 256− 258. (f) Teranishi, T.; Kiyokawa, I.; Miyake, M. *Adv. Mater.* **1998**, *10*, 596−599. (g) Whetten, R. L.; Khoury, J. T.; Alvarez, M. M.; Murthy, S.; Vezmar, I.; Wang, Z. L. Stephens, P. W.; Clevelend, C. L.; Luedtke, W. D.; Landman, U. *Adv. Mater.* **1996**, *8*, 428−433. (h) Schaaff, T. G.; Knighjt, G.; Shafigullin, M. N.; Borkman, R. F.; Whetten, R. L. *J. Phys. Chem. B* **1998**, *102*, 10643−10646.

(3) (a) Hostetler, M. J.; Stokes, J. J.; Murray, R. W. *Langmuir* **1996**, *12*, 3604−3612. (b) Badia, A.; Singh, S.; Demers, L.; Cuccia, L.; Brown, G. R.; Lennox, R. B. *Chem. Eur. J.* **1996**, *2*, 359−363. (c) Badia, A.; Cuccia, L.; Demers, L.; Morin, F.; Lennox, R. B. *J. Am. Chem. Soc.* **1997**, *119*, 2682−2692. (d) Brust, M.; Fink, J.; Bethell, D.; Schiffrin, D. J.; Kiely, C. *J. Chem. Soc., Chem. Commun.* **1995**, 1655−1656. (e) Templeton, A. C.; Hostetler, M. J.; Kraft, C. T.; Murray, R. W. *J. Am. Chem. Soc.* **1998**, *120*, 1906−1911. (f) Ingram, R. S.; Hostetler, M. J.; Murray, R. W. *J. Am. Chem. Soc.* **1997**, *119*, 9175−9178. (g) Templeton, A. C.; Hostetler, M. J.; Warmoth, E. K.; Chen, S.; Hartshorn, C. M.; Krishnamurthy, V. M.; Forbes, M. D. E.; Murray, R. W. *J. Am. Chem. Soc.* **1998**, *120*, 4845−4849. (h) Arnold, R. J.; Reilly, J. P. *J. Am. Chem. Soc.* **1998**, *120*, 1528−1532. (i) Connolly, S.; Fullam, S.; Korgel, B.; Fitzmaurice, D. *J. Am. Chem. Soc.* **1998**; *120*, 2969−2970.

(4) (a) Collier, C. P.; Vossmeyer, T.; Heath, J. R. *Annu. Rev. Phys. Chem.* **1998**, *49*, 371−404. (b) Heath, J. R.; Knobler, C. M.; Leff, D. V. *J. Phys. Chem. B* **1997**, *101*, 189−197. (c) Harfenist, S. A.; Wang, Z. L.; Alvarez, M. M.; Vezmar, I.; Whetten, R. L. *J. Phys. Chem.* **1996**, *100*, 13904−13910. (d) Wang, Z. L. *Adv. Mater.* **1998**, *10,* 13−30. (e) Lin, X. M.; Sorensen, C. M.; Klabunde, K. J. *Chem. Mater.* **1999**, *11*, 198−202. (f) Wang, Z. L.; Harfenist, S. A.; Vezmar, I.; Whetten, R. L.; Bently, J.; Evans, N. D.; Alexander, K. B. *Adv. Mater.* **1998**, *10*, 808− 812. (g) Harfenist, S. A.; Wang, Z. L.; Whetten, R. L.; Vezmar, I.; Alvarez, M. M. *Adv. Mater.* **1997**, *9*, 817−822. (h) Korgel, B. A.; Fullam, S.; Connolly, S.; Fitzmaurice, D. *J. Phys. Chem. B* **1998**, *102*, 8379− 8388. (i) Luedtke, W. D.; Landman, U. *J. Phys. Chem.* **1996**, *100*, 13323−13329. (j) Wang, Z. L.; Harfenist, S. A.; Whetten, R. L.; Bently, J.; Evans, N. D. *J. Phys. Chem. B* **1998**, *102*, 3068−3072. (k) Korgel, B. A.; Fitzmaurice, D. *Phys. Rev. B* **1999**, *59*, 14191−14201.

cluster surfaces has been seen by molecular dynamics calculations also.[4i] There are, however, other studies, which indicate that the chains appear to fill the void volume between the clusters and the density and not the extended length of the chains determine the interparticle distance.[4k] Thus, apart from the interchain van der Waals interaction, deformations in the alkyl chain body due to space filling also contribute to intercluster association. Additional interactions through the cluster cores can also occur.[4k]

Ordered superlattices composed of micrometer-sized particles have been known in colloid chemistry for a long time, but there are only a few examples for the crystallization of metal nanoparticles.[4] We have recently synthesized a number of alkanethiol-protected silver clusters which crystallize to form single-phase superstructures.[5] These monolayer assembled cluster solids have been investigated with a variety of analytical methods.[5] The studies suggest that these materials are true molecular solids possessing distinct melting points in their phase diagrams suggesting that the constituent clusters are molecules.[5,6]

Several groups have reported bimetallic alloy nanoclusters with different combinations of metals.[7] Isolated monolayer protected alloy clusters (MPACs) of AuAg have been the subject of earlier reports by Hostetler et al.[8] and Kim et al.[9a] Although a variety of studies have been reported for MPC superlattices,[4] to the best of our knowledge, no report exists on MPAC superstructures. For the past several years, we have been exploring the properties of planar monolayers by surface enhanced Raman spectroscopy[10] and ion/surface scattering.[11] The possibility of extending our investigations with more conventional techniques, made us choose monolayers on cluster surfaces for later studies.[12] Intercluster interactions through monolayers make it possible to prepare three-dimensional solids of clusters.[5] We decided to extent this investigation to alloy cluster systems, principally to examine the differences between them and the pure metal clusters.

In this paper, we show that AuAg alloy clusters protected with octadecanethiol (ODT) monolayers form crystalline solids over a range of cluster compositions. *These crystalline solids are not superlattices in the conventional sense since no appropriate sublattice exists.* They can be described better as crystalline solids of monolayer protected clusters (CS-MPCs) or crystalline solids of monolayer protected alloy clusters (CS-MPACs). The metal atoms and the monolayers within a cluster possess translational periodicity as in the bulk metal and in the alkane solid, respectively. The solids and the isolated clusters in solution have been investigated by a variety of spectroscopic and calorimetric techniques.

Experimental Section

The methodology used for the synthesis of CS-MPACs is almost the same as that reported for CS-MPCs.[5] These alloy clusters were prepared by reducing a mixture of gold (in the form of $HAuCl_4 \cdot 3H_2O$) and silver (in the form of $AgNO_3$). Alloy clusters with silver mole fractions (x_{Ag}) of 0.33, 0.66, and 0.75 were prepared. These clusters are designated as $AuAg_n$ (n = 0.5, 2, and 3 corresponding to the ratio of the (Ag:Au) mole fractions) in the following discussion. Since it was known from our earlier studies that ODT-protected clusters form of CS-MPCs with a well-defined melting point,[6] CS-MPACs were prepared only with this thiol. An aqueous solution of $HAuCl_4$ was added to a vigorously stirred aqueous solution of $AgNO_3$ (keeping the total volume as 20 mL). Stirring was continued for 5 min and a 0.0358 M toluene solution (42 mL) of tetra *n*-octylammonium bromide was added. The precipitate of AgCl formed initially disappeared, indicating the complete phase transfer of the metal ions. After 1 h of stirring, a 0.0139 M toluene solution (47 mL) of octadecanethiol was added followed by a 16.5 mL aqueous solution (0.2378 M) of sodium borohydride over a period of several minutes. The solution was stirred overnight, and the organic layer was separated. It was allowed to evaporate slowly to 10 mL at the ambient temperature, and 100 mL of methanol was added to precipitate the cluster. The precipitate was allowed to settle and was collected by centrifuging. The material was washed several times with methanol to remove unreacted thiol and phase-transfer reagent and was air-dried. For comparison, we prepared ODT-protected Au and Ag clusters by separate reduction using the same procedure as above. The resulting cluster solutions were mixed and stirred for 12 h to attain thermodynamic equilibrium and a crystalline solid was formed by slow evaporation of the toluene solution. All the clusters and monolayer-assembled cluster solids were completely soluble in nonpolar solvents. When the solids were exposed for long periods to air, solubility decreased and sonication was necessary for complete dissolution. The complete solubility in nonpolar solvents indicates the absence of Au[13] and Ag-thiolates[14] in the solid, which are insoluble. IR, UV, and DSC signatures also confirm the absence of thiolates, which have been independently investigated.[6]

X-ray diffractograms with Co Kα radiations were measured in a Philips D1 X-ray diffractometer at room temperature for

(5) Sandhyarani, N.; Resmi, M. R.; Unnikrishnan, R.; Shuguang Ma; Vidyasagar, K.; Antony, M. P.; Panneer Selvam, G.; Visalakshi, V.; Chandrakumar, N.; K. Pandian; Tao, Y.-T.; Pradeep, T. *Chem. Mater.* **2000**, *12*, 104−113.

(6) (a) Sandhyarani, N; Antony, M. P.; Panneer Selvam, G.; Pradeep, T. *Chem. Eur. J.*, submitted for publication. (b) Sandhyarani, N.; Pradeep, T.; Chakrabarti, J. Yousuf, M.; Sahu, H. K *Phys. Rev. B.*, in press.

(7) (a) Henglein, A.; Giersig, M. J. *J. Phys. Chem.* **1994**, *98*, 6931−6937. (b) Schwank, J. *Gold Bull.* **1983**, *16*, 98−102. (c) Schwank, J. *Gold Bull.* **1983**, *16*, 103−107.

(8) Hostetler, M. J.; Zhong, C.-J.; Yen, B. K. H.; Anderegg, J.; Gross, S. M.; Evans, N. D.; Porter, M.; Murray, R. W. *J. Am. Chem. Soc.* **1998**, *120*, 9396−9397.

(9) (a) Han, S. W.; Kim, Y.; Kim, K. *J. Colloid Interface Sci.* **1998**, *208*, 272−278. (b) Link, S.; Wang, Z. L.; El-Sayed, M. A. *J. Phys. Chem. B* **1999**, *103*, 3529−3533. (c) Mulvaney, P. *Langmuir* **1996**, *12*, 788−800.

(10) (a) Sandhyarani, N.; Murty, K. V. G. K.; Pradeep, T. *J. Raman Spectrosc.* **1998**, *29*, 359−363. (b) Sandhyarani, N.; Pradeep, T. *Vacuum* **1998**, *49*, 279−284. (c) Murty, K. V. G. K.; Venkataramanan, M.; Pradeep, T. *Langmuir* **1998**, *14*, 5446−5456. (d) Sandhyarani, N.; Skanth, G.; Berchmans, S.; Yegnaraman, V.; Pradeep, T. *J. Colloid Interface Sci.* **1999**, *209*, 154−161. (e) Sandhyarani, N.; Pradeep, T. *J. Colloid Interface Sci.* **1999**, *218*, 176−183. (f) Venkataramanan, M.; Skanth, G.; Bandyopadhyay, K.; Vijayamohanan, K.; Pradeep, T. *J. Colloid Interface Sci.* **1999**, *212*, 553−561. (g) Venkataramanan, M.; Murty, K. V. G. K.; Pradeep, T.; Deepali, W.; Vijayamohanan, K. *Langmuir*, in press. (h) Berchmans, S.; Yegnaraman, V.; Sandhyarani, N.; Murty, K. V. G. K.; T. Pradeep, T. *J. Electroanal. Chem.* **1999**, *468*, 170−174. (i) Bandyopadhyay, K.; Vijayamohanan, K.; Venkataramanan, M.; Pradeep, T. *Langmuir* **1999**, *15*, 5314−5319.

(11) (a) Pradeep, T.; Ast, T.; Cooks, R. G.; Feng, B. *J. Phys. Chem.* **1994**, *98*, 9301−9309. (b) Pradeep, T.; Riederer, D. E., Jr.; Hoke, S. H.; Ast, T.; Cooks, R. G.; Linford, M. R. *J. Am. Chem. Soc.* **1994**, *116*, 8658−8665. (c) Cooks, R. G.; Ast, T.; Pradeep, T.; Wysocki, V. H. *Acc. Chem. Res.* **1994**, *27*, 316−321. (d) Pradeep, T.; Patrick, J. S.; Feng, B.; Ast, T.; Miller, S. A.; Cooks, R. G. *J. Phys. Chem.* **1995**, *99*, 2941−2944. (e) Pradeep, T.; Evans, C.; Shen, J.; Cooks, R. G. *J. Phys. Chem. B* **1999**, *103*, 5304−5310. (f) Pradeep, T.; Shen, J.; Evans C.; Cooks, R. G. *Anal. Chem.* **1999**, *71*, 3311−3317.

(12) (a) Venkataraman, M.; Ma, S.; Pradeep, T. *J. Coll. Interface Sci.* **1999**, *216*, 134−142. (b) Resmi, M. R.; Sandhyarani, N.; Unnikrishnan, R.; Ma, S.; Pradeep, T. *J. Colloid Interface Sci.* **1999**, *217*, 395−402. (c) Sandhyarani, N.; Pradeep, T. *J. Mater. Chem.* **2000**, *10*, 981−986.

(13) XPS of Au alkanethiolate is given in: McNeillie, A.; Brown, D. H.; Smith, W. E.; Gibson, M.; Watson, L. *J. Chem. Soc., Dalton Trans.* **1980**, 767−770.

ascertaining the formation of CS-MPACs as well for determining the mean cluster diameters. The samples were spread on antireflection glass slides to give uniform films. The films were wetted with acetone for uniformity and were blown dry before measurement. All samples were similarly prepared. Peaks were indexed with the AUTOX-93 program. Optical absorption spectra were collected with a Varian Cary 5 UV/vis/NIR spectrophotometer. Solutions were prepared in toluene and chloroform. The transmission electron microscopic (TEM) measurements were performed with a Philips 120 kV machine. Drop-cast films of the clusters were prepared on carbon-coated Cu grids. XPS measurements were carried out with a VG ESCALAB Mk II spectrometer with Mg Kα radiation. X-ray flux was kept low (electron power: 70 W) in order to avoid beam induced damage.[15] Acquisition took about 15 min for each core level. All regions, C 1s, S 2p, O 1s, and Ag 3d and Au 4f were measured with 100 eV pass energy. The measurements were carried out under a pressure of 10^{-8} Torr. Thick films of the samples (spread on nickel sample stubs) were used for the measurements. Infrared spectra were measured with a Bruker IFS 66v FT-IR spectrometer. Samples were prepared in the form of KBr pellets. All spectra were measured with a resolution of 4 cm^{-1} and were averaged over 200 scans. Variable-temperature spectra were measured with a home-built heater with a programmable temperature controller. Differential scanning calorimetric (DSC) data were taken with a Netzsch PHOENIX DSC204 instrument. A total of 10 mg of the samples encapsulated in aluminum pans was used. The measurements were conducted in the temperature range of 293−473 K. A scan speed of 10 K/min was used in the measurements. Thermogravimetric (TG) data were acquired with a Netzsch STA 409 instrument. About 10 mg of the sample was used for each measurement. Data in the range of 303−923 K were measured. A scan speed of 20 K/min was used in these measurements. The samples left behind after TG analysis were metal powders.

Elemental compositions of the clusters were determined using inductively coupled plasma atomic emission spectrometry (ICP AES). The different alloy samples were digested with aqua regia to dissolve Au and the metal ion concentrations were measured with ICP AES. Ag compositions were calculated from the total alloy masses determined by TG and the corresponding Au compositions measured by ICP AES (accuracy for Au measurement was ±0.02 wt %).

Results and Discussion

In Figure 1 we show the Co Kα X-ray diffractograms of all the compositions studied. All the compositions, especially the Ag-rich ones, show reflections other than (111), (200), and (220) reflections of silver or gold (both occur at the same position). All the spectra show characteristic low angle peaks corresponding to larger unit cells. Such a lattice composed of alkanethiolate protected clusters can only result from the periodic arrangement of these clusters. The broad peaks centered at 44.9 ± 0.20° and 51.8 ± 0.20° are due to the bulk Au and Ag (the peak positions are the same for both) and the width of any of their peaks can be used to find the average cluster size. Scherrer formula[16] gives the diameters of the particles as 26, 20, and 21 Å for AuAg$_{0.5}$,

(14) (a) Bensebaa, F.; Ellis, T. H.; Kruus, E.; Voicu, R.; Zhou, Y. *Langmuir* **1998**, *14*, 6579−6587. (b) Parikh, A. N.; Gillmor, S. D.; Beers, J. D.; Beardmore, K. M.; Cutts, R. W.; Swanson, B. I. *J. Phys. Chem.* **1999**, *103*, 2850−2861. (c) Dance, I. G.; Fisher, K. J.; Herath Bamda, R. M.; Scudder, M. L. *Inorg. Chem.* **1991**, *30*, 183−187. (d) Beana, M. J.; Espinet, P.; Lequerica, M. C.; Levelut, A. M. *J. Am. Chem. Soc.* **1992**, *114*, 4182−4185. (e) Fijolek, H. G.; Grohal, J. R.; Sample, J. L.; Natan, M. J. *Inorg. Chem.* **1997**, *36*, 622−628.

(15) Colvin, V. L.; Goldstein, A. N.; Alivisatos, A. P. *J. Am. Chem. Soc.* **1992**, *114*, 5221−5230.

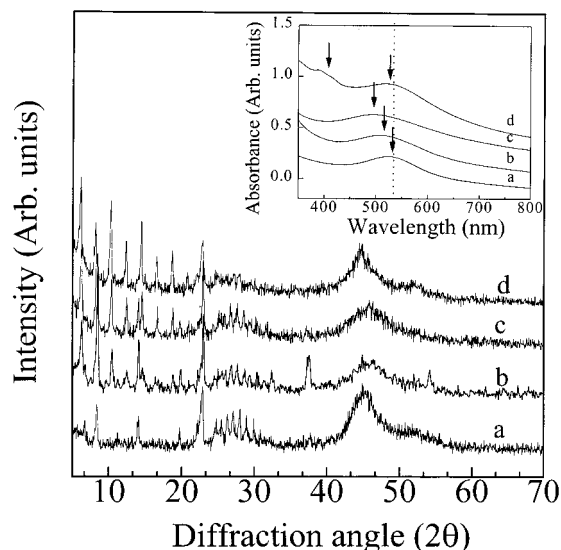(16) West, A. R. *Solid State Chemistry and its Applications*; John Wiley and Sons: New York, 1987.

Figure 1. The Co Kα-induced powder diffraction patterns of the AuAg alloy clusters protected with octadecanethiol. Ag mole fractions are 0.33, 0.66, and 0.75 for a, b, and c, respectively. Diffractogram d corresponds to the mixed cluster sample prepared by separate reduction. The peak positions, assignments, and unit cell dimensions are presented in Table 1. Inset shows the optical absorption spectra of AuAg alloy clusters protected with octadecanethiol. Ag mole fractions are 0.33, 0.66, and 0.75 for a, b, and c, respectively. Spectrum d corresponds to the mixed cluster sample prepared by separate reduction. Peak maxima are indicated. The ordinate scale corresponds to spectrum a and other spectra are offset for clarity.

Table 1. XRD Peak Positions (Low Angle), Assignments, and Unit Cell Dimensions of the Solids of Octadecanethiolate Protected Alloy Clusters

AuAg$_{0.5}$ $a = 63.92^b$		AuAg$_2$ $a = 71.67^b$		AuAg$_3$ $a = 73.90^b$		AuAg^a $a = 78.72^b$	
$2\theta^c$	(*hkl*)	$2\theta^c$	(*hkl*)	$2\theta^c$	(*hkl*)	$2\theta^c$	(*hkl*)
6.80	(330)	6.23	(331)	6.21	(420)	6.11	(332)
8.35	(511)	8.48	(531)	8.32	(600)	8.24	(620)
14.20	(752)	10.51	(721)	10.38	(642)	10.30	(651)
19.79	(1071)	12.53	(662)	12.47	(840)	12.38	(930)
22.84	($1\overline{4}20$)	14.21	(770)	14.08	(1011)	14.50	(1111)
24.78	($1\overline{5}31$)	18.86	(1066)	14.59	($1\overline{0}31$)	16.58	($1\overline{2}41$)
25.35	($1\overline{4}71$)	19.86	($1\overline{0}93$)	16.71	($1\overline{2}00$)	18.71	($1\overline{4}22$)
26.33	($1\overline{6}30$)	23.00	($1\overline{5}52$)	18.83	($1\overline{0}91$)	20.75	($1\overline{5}51$)
27.13	($1\overline{6}50$)	25.64	($1\overline{7}51$)	19.76	($1\overline{4}21$)	22.83	($1\overline{2}\,12\,4$)
28.06	($1\overline{4}\,10\,2$)	26.81	($1\overline{6}85$)	22.95	($1\overline{3}\,10\,1$)		
28.93	($1\overline{4}\,11\,1$)	27.71	($1\overline{5}\,12\,0$)	25.92	($1\overline{8}42$)		
29.96	($1\overline{8}4\overline{1}$)	28.66	($1\overline{4}\,14\,1$)	26.70	($1\overline{8}62$)		
30.89	($1\overline{9}10$)	30.34	($2\overline{0}62$)	27.69	($1\overline{7}\,10\,1$)		
		32.42	($2\overline{2}40$)	28.59	($2\overline{0}40$)		
		37.56	($2\overline{5}62$)	30.31	($2\overline{1}50$)		
				31.69	($2\overline{2}50$)		

^{a} Corresponds to a superstructure made from separately prepared Au and Ag clusters protected with ODT. ^{b} Unit cell dimensions in Å. The true unit cells could be integral multiples of the lattice parameters given here. There are peaks below 5° and small-angle X-ray scattering is necessary to obtain the exact lattice parameters and is not the focus of this paper. ^{c} In degrees. Standard deviation ±0.20°.

AuAg$_2$, and AuAg$_3$ clusters. Diffractograms of the 1:2 and 1:3 compositions (AuAg$_2$ and AuAg$_3$) are very similar and can be indexed to single cubic unit cells. The unit cell dimensions and assignments are given in Table 1.

A particularly noticeable fact is that whereas the isolated cluster peaks are broad, the small angle reflec-

tions are narrow indicating that the domain sizes of the superstructures are large. In our earlier study of single-phase superlattices of Ag clusters,[5] it was noted that even the bulk silver reflections were narrow although the average cluster size from transmission electron microscopy (TEM) investigations was 4 ± 0.5 nm. This indicates that bulk reflections also become part of the superlattice reflections and the crystallites are large in size.[5] The width of the peaks give a dimension of about 240 nm, indicating that there are several unit cells in each crystallite.

From TEM investigations it is clear that the particle size distribution is narrow (4 ± 0.5 nm), as in the cases of isolated clusters of Ag superlattices.[5] About 50 particles were considered for obtaining the distribution. Au clusters give a smaller particle size distribution (3 ± 0.5 nm) under identical synthetic conditions. Earlier studies of alloy clusters, under similar conditions also give a narrow size distribution.[8] In the TEM of CS-MPACs, a periodic assembly was not observed. We believe that the organics assembled crystallites melt under electron beam as in the case of Ag cluster superlattices.[5]

The superstructures were found to be more stable in Ag-rich compositions. As reported before, pure Au clusters are not ideal candidates for the formation of superlattices[5] by this synthetic procedure. Earlier study[8] suggests the incorporation of more noble metal to the alloy cluster core. Galvanic effects are suggested[8] to play a part in the differential incorporation.

The solid prepared by mixing separately prepared AuODT and AgODT also yielded a single cubic unit cell with similar lattice constants (Table 1). The XRD pattern (Figure 1d) is almost similar to that of $AuAg_3$ (Figure 1c). However, it is significantly different from the AgODT superlattice.[5] This mixed lattice can be assumed to be an intercalation of Au clusters into the Ag superlattice. Variation in the structure with varying composition is under investigation currently.

Inset of Figure 1 shows the optical absorption spectra of the alloy cluster solutions in chloroform. The traces a, b, and c correspond to the nominal compositions, 1:0.5, 1:2, and 1:3 ($AuAg_{0.5}$, $AuAg_2$, and $AuAg_3$ clusters, respectively). The concentrations (in weight) in the different cluster solutions are almost comparable, and the intensities are presented without manipulation except for the offset for clarity. The alloy clusters show an intense surface plasmon (SP) absorption band whose peak maximum is directly related to the core composition as reported before.[8,9] Gold and silver clusters protected with ODT give peak maxima around 520[2c] and 420 nm,[17] respectively. The maxima of the alloy clusters fall between and the peaks red shift with increasing Au content. This is consistent with the literature data.[8] From the absorption spectra, we obtain the true core compositions of our clusters as 1:0.33, 1:0.87, and 1:1.55 for $AuAg_{0.5}$, $AuAg_2$, and $AuAg_3$, respectively. This is also in rough agreement with the compositions derived from Au/Ag intensities in XPS and elemental analyses (see below). No preparation gave multiple SP bands. In contrast, a mixture of Au and Ag clusters (a solution of AuODT-AgODT mixed cluster solid) gave peaks corre-
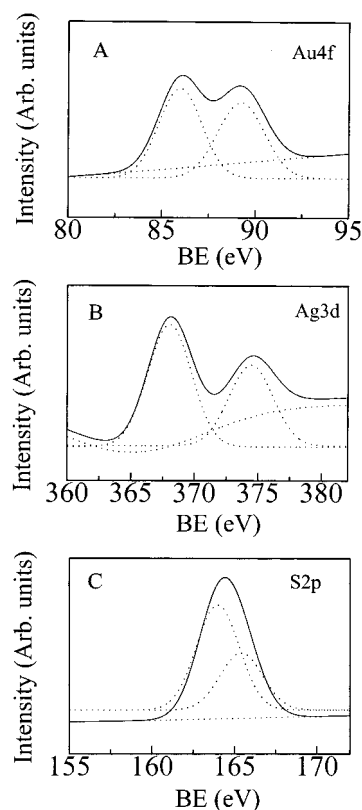

Figure 2. X-ray photoelectron spectra of (a) Au 4f, (b) Ag 3d, and (c) S 2p regions of $AuAg_{0.5}$ cluster. The peaks are fitted with Gaussians. The full lines are the composite fits and the dotted lines are the components. For Au and Ag regions, a background function is also added.

sponding to both clusters (spectrum d). This indicates that in the alloy cluster preparation, no separate Au and Ag clusters are forming, although it is known that phase segregation of nanoparticles occur.[18]

True bulk compositions of the alloy clusters were determined by atomic emission spectroscopy. These analyses give a composition of 1:0.43, 1:1.16, and 1:2.19 for $AuAg_{0.5}$, $AuAg_2$, and $AuAg_3$ respectively, suggesting preferential incorporation of gold in the cluster.

Figure 2 shows the X-ray photoelectron spectra of Au 4f, Ag 3d, and S 2p regions of the $AuAg_{0.5}$ sample. XPS show binding energies corresponding to Au(0)[19] and Ag(0)[19] for all the clusters investigated. Au $4f_{7/2}$ and Ag $3d_{5/2}$ occur at 84.0 and 368.0 eV binding energy. Intensities of the Ag and Au peaks can be used to find out the bulk compositions of the clusters. The calculated compositions are 1:0.562, 1:1.373, and 1:1.904, respectively for $AuAg_{0.5}$, $AuAg_2$, and $AuAg_3$. The data agree well with those obtained from absorption measurements and the results of Hostetler et al.[8] S 2p region gives only a well-defined single peak for the clusters, unlike that reported by Hostetler et al. probably due to poor resolution ($\sim$1 eV). Even after several hours of X-ray exposure, no beam-induced damaged products[15] were observed. There are small differences in the peak maxima within 0.7 eV, which we attribute to the possible differences in the

(18) Kiely, C. J.; Fink, J.; Brust, M.; Bethel, D.; Schiffrin, D. J. *Nature* **1998**, *396*, 444–446.
(19) Briggs, D.; Seah, M. D. *Practical Surface Analysis by Auger and X-ray Photoelectron Spectroscopy*; John Wiley and Sons: Chichester, 1984.

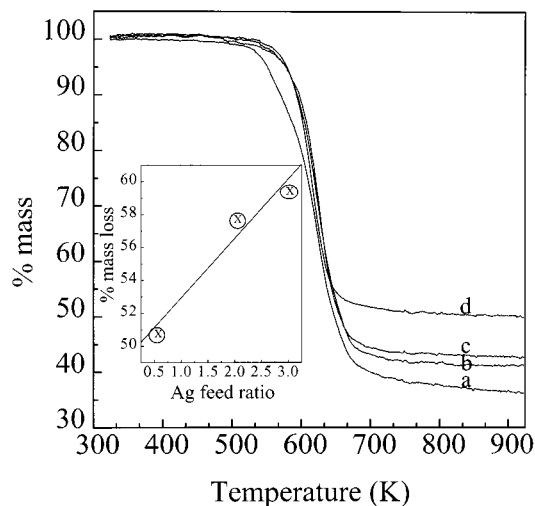(17) Kang, S. Y.; Kim, K. *Langmuir* **1998**, *14*, 226–230.

Figure 3. Thermogravimetric data of the AuAg alloy clusters (a) corresponds to separate reduction and b, c, and d are for alloy clusters with Ag mole fractions 0.75, 0.66, and 0.33, respectively. Inset shows a linear fit of the plot of percentage mass losses vs the Ag feed ratio.

binding on Au and Ag sites on the alloy surface. C 1s appears as a single distinct peak at 285 eV.

Thermogravimetric data reveal weight losses between pure Au and Ag clusters. Whereas AuODT shows a weight loss of 31%, it is 64% in the corresponding Ag cluster.[5] In all the alloy clusters investigated, the weight loss is greater than that of pure gold and it increases with the Ag content. Thermogravimetric data of the alloy clusters are presented in Figure 3 and a plot of the weight loss with the metal salt feed ratio is shown in the inset. Since the cluster sizes are similar for all these compositions (from TEM and XRD), it can be suggested that Ag concentration is determining the coverage. A larger coverage increases the possibility of superstructure formation. It may be noted that whereas it is possible to form single-phase superstructures with Ag for a range of alkanethiols, only a small fraction (<5%) of the solid is in this form for Au.[5]

There is only one distinct weight loss observed for all the compositions studied and there is no change in the desorption temperature with varying composition. We take this observation to mean that the surface is an intimate mixture of Au and Ag sites and no Au and Ag islands are present on the cluster surface. The energetics of chemisorption on Au and Ag sites on the alloy surfaces are comparable yielding a single desorption transition.

Differential scanning calorimetric traces of the solids show two distinct first-order transitions. The first corresponds to the melting of the alkanethiolate chain assembly and the second corresponds to the melting of the superstructure.[5] All the alloy clusters show very similar DSC traces and a representative measurement corresponding to AuAg$_3$ is shown in Figure 4A. Trace B corresponds to the mixed cluster solid. Two cycles of measurements were done on all the samples. The sample was first heated from 293 to 423 K and cooled back to 293 K (experiment 1) and then (the same sample) was heated to 473 K and cooled back to 293 K (experiment 2). The trace corresponding to the first cycle is shown as the broken line curve and the full line corresponds to the second cycle. In experiment 1, the
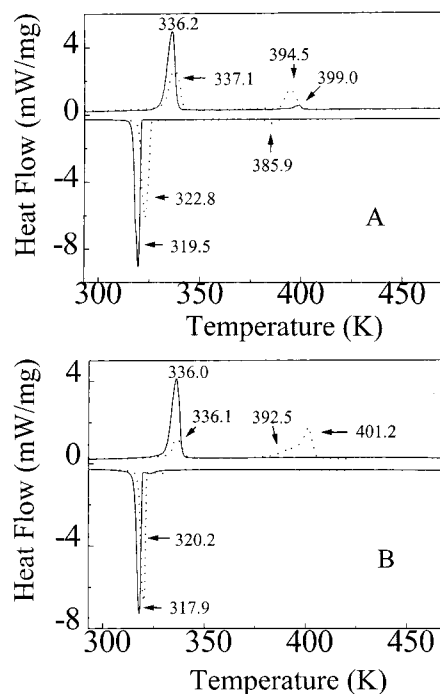

Figure 4. Differential scanning calorimetric traces of (A) AuAg$_3$ and (B) AuAg mixed cluster solid. Two separate cycles are indicated by dashed lines (- - -) and full lines (—). The former corresponds to heating to 423 K and cooling back to 293 K and the later corresponds to heating to 473 K and cooling back to 293 K. Heating/cooling rate was 10 K/min. Transition temperatures and enthalpies are given in Table 2.

alkyl chain melting is manifested at around 337.1 K with a transition enthalpy of 89.8 J/gram for the AuAg$_3$ cluster. Alkyl chain melting appears in the infrared spectrum also at a similar temperature. The superstructure melting is seen at 394.5 K with an enthalpy of 47.0 J/gram. *Both these transitions are manifested in the reverse direction also*, enthalpy of the alkyl chain melting is higher, whereas the other has been reduced substantially. Both these show histeresis, characteristic of first-order transitions. During the second cycle, the alkyl chain melting transition appears at the same temperature and the enthalpy is comparable to that of the previous cooling curve. The melting of the superstructure is again manifested with an enthalpy comparable to the previous cooling curve. Upon return, only the alkyl chain freezing transition is manifested.

The results are in agreement with the phase transitions of Ag superlattices investigated earlier.[5] It has been shown that the superlattice liquid can come back to the original order, if cooled from a temperature near to the melting point.[6] It appears that in a narrow window of temperatures, the cluster molecule with the alkyl chain assembly does not possess much orientational freedom in the liquid state and upon cooling, it is possible to regain the translational order. However, at higher temperatures, orientational freedom of the cluster molecules increases and interdigitation of the alkyl chain[4d,h] bundles is not possible. IR and DSC studies suggested that upon repeated annealing, alkyl chain assembly becomes more ordered (packing order increases), which contributes to a reduction in the amount of the superstructure solid.[6] There could be additional factors responsible for the observed phenomena such as aggregation of clusters. In the case of

1760   *Chem. Mater., Vol. 12, No. 6, 2000*

Sandhyarani and Pradeep

Table 2. Enthalpies and Transition Temperatures of the Octadecanethiolate Protected AuAg Alloy Cluster Solids (from DSC) upon Repeated Heating/Cooling Cycles[a]

composition		AuAg$_{0.5}$	AuAg$_2$	AuAg$_3$	AuAg[b]
I heating	ΔH_1 (J/g)	111.6	68.1	89.8	31.0
from 293 K	T_1(K)	337.0	336.6	337.1	336.1
	ΔH_2 (J/g)	2.9	24.1	47.0	75.8
	T_2 (K)	381.8	395.1	394.5	392.5
	T_3 (K)[c]				401.2
I cooling	ΔH_1 (J/g)	128.5	127.9	134.7	102.9
from 423 K	T_1 (K)	324.8	321.4	322.8	320.2
	ΔH_2 (J/g)			4.1	
	T_2 (K)			385.9	
II heating	ΔH_1 (J/g)	129.3	128.7	135.0	116.1
from 293 K	T_1 (K)	336.5	335.8	336.2	336.0
	ΔH_2 (J/g)			4.8	
	T_2 (K)			399.0	
IIcooling	ΔH_1 (J/g)	126.2	133.4	148.8	103.9
from 473 K	T_1 (K)	322.0	320.8	319.5	317.9
	ΔH_2 (J/g)				
	T_2 (K)				

[a] T_1 and T_2 are transition temperatures corresponding to alkyl chain melting and superstructure melting. ΔH_1 and ΔH_2 are corresponding enthalpies. [b] Mixed-metal cluster superstructure solid. [c] Multiple transitions, T_2 and T_3 are observed for the mixed cluster solid but ΔH_2 is the sum of these two transitions.

AgODT, this has been observed in TEM.[5] The DSC data are summarized in Table 2.

In the mixed-metal solid, the alkyl chain transition occurs at the same temperature as in the alloy metal case, but the superstructure melting transition occurs through multiple steps (Figure 4B). This appears to be due to the various conformations of the alkyl chains present in the interdigitated state. *Upon cooling back from 423 K, the superstructure freezing transition is not manifested*. In the second cycle, only the alkyl chain melting is seen.

To find the similarity and the differences in the alkyl chain assembly, infrared spectra of the samples were investigated. In Figure 5 A and B, the high and low-frequency region of the infrared spectra of the samples are shown. The positions of the characteristic peaks are the same in all the samples. The methylene symmetric and antisymmetric (d$^+$ and d$^-$) and the methyl symmetric and antisymmetric (r$^+$ and r$^-$) peaks occur at the same positions. The methylene peaks are at 2920 and 2849 cm^{-1}, characteristic of crystalline alkanes.[20] The peak shapes of all the spectra are identical indicating similarity in the environment.

In the low-frequency region, the prominent peaks correspond to the methylene wagging and the rocking bands around 1460 and 720 cm^{-1}, in addition to a number of progression bands. The 720 cm^{-1} band has also contributions from the C$-$S$_T$ stretching mode, which is not clearly manifested. The interesting aspect to note is that as the Au content increases, as in AuAg$_{0.5}$, the methylene wagging and rocking bands split into two, with almost equal intensity, which is attributed to factor group splitting suggested to be due to interchain interactions present in the solid.[21] Similar splitting is encountered in the orthorhombic and monoclinic struc-
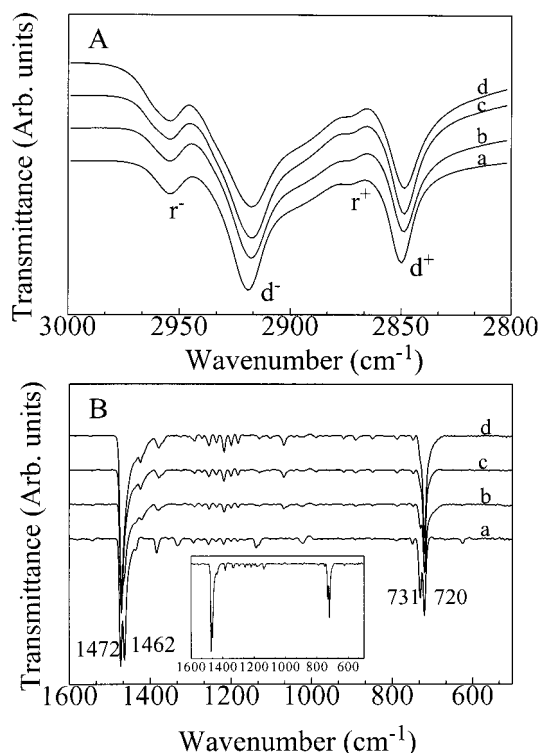

Figure 5. High (A) and low (B) frequency FT-IR spectra of the alloy clusters protected with octadecanethiol: (a) AuAg$_{0.5}$, (b) AuAg$_2$, and (c) AuAg$_3$. Spectrum d corresponds to the mixed cluster. Note the splitting of the 720 cm^{-1} band in spectrum a. Inset shows the low-frequency region of the FT-IR spectrum of AuAg$_{0.5}$ after annealing at 473 K.

tures of crystalline alkanes,[22,23] which are generally the low-temperature phases. In spectrum of monolayers on planar surfaces also, a similar splitting is seen at 80 K.[24] In the present spectrum, peaks in the methylene wagging region appear at 1472 and 1462 cm^{-1} and the rocking modes appear at 731 and 720 cm^{-1}, respectively. The splitting of the methylene rocking mode at a mean value of 725 cm^{-1} is characteristic of a monoclinic unit cell bearing even number of carbon atoms.[22] In this case, the weaker component is always on the higher frequency side, whereas in orthorhombic structure, intensities of both the peaks are similar. The two peaks in the methylene bending region are also of similar intensities. This spectral pattern, with nearly equal intensity component peaks, is seen in monolayer protected Ag clusters upon repeated annealing.[6a] It may be noted that in the case of pure Au clusters, the factor group splitting is less marked and the component peaks show dissimilar intensities. The two peaks are present in other alloy compositions also, in varying intensity, suggesting that interchain interactions are present in different extent. In the case of Ag-rich compositions where factor group splitting is not evident, it appears upon annealing. For Au-rich compositions, this annealing did not make a difference in the spectral pattern as seen in the inset where the spectrum of AuAg$_{0.5}$ after a 473 K annealing is shown. For this experiment, we heated the sample to 473 K in air and cooled back. This sample was pressed

(20) (a) Snyder, R. G.; Strauss, H. L.; Elliger, C. A. *J. Phys. Chem.***1982**, *86*, 5145−5150. (b) Snyder, R. G.; Maroncelli, M.; Strauss, H. L.; Hallmark, V. M. *J. Phys. Chem.***1986**, *90*, 5623−5630.

(21) Colthup, N. B.; Daly, L. H.; Wiberley, S. E. *Introduction to Infrared and Raman Spectroscopy*; Academic Press: New York, 1975; p 232.

(22) Snyder, R. G. *J. Mol. Spectrosc.* **1961**, *7*, 116−144.

(23) Nielsen, J. R.; Hathaway, C. E. *J. Mol. Spectrosc.* **1963**, *10*, 366−377.

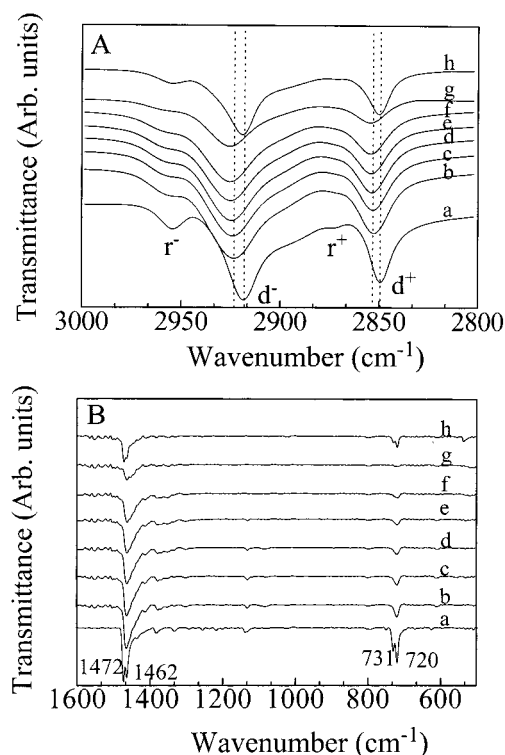(24) Dubois, L. H.; Nuzzo, R. G. *Annu. Rev. Phys. Chem.* **1992**, *43*, 437−463.

Figure 6. Variable-temperature FT-IR spectra of the AuAg$_{0.33}$ alloy cluster in the high (A) and low (B) frequency regions. Temperatures are (a) 298, (b) 323, (c) 348, (d) 373, (e) 398, (f) 423, and (g) 448 K. Spectrum h shows the data after cooling back from 448 K. Note that the factor group splitting re-appeared in spectrum h.

with KBr, and the IR spectrum was measured. Annealing did not make any difference in the C–H stretching positions, but the peaks narrowed after annealing indicating increased order in the alkyl chain body.

To investigate whether the phase transition of the monolayer on the alloy cluster is same as in the case of the parent metal clusters, we performed a variable temperature IR study. In this experiment, we heated the pressed KBr pellets in situ in the spectrometer. Figure 6 A and B present the variable-temperature IR data of AuAg$_{0.5}$ in the (A) high- and (B) low-frequency regions. At room temperature, this cluster shows a factor group splitting of the methylene rocking and wagging modes. At 323 K, it undergoes a sudden transition in which the factor group splitting disappeared along with the blue shift of the C–H stretching modes. The shift in C–H stretching frequency indicates melting of the alkyl chains. It is to be noted that in the pure Ag clusters we observed the melting of the alkyl chain at still higher temperatures.[6a] Other alloy cluster solids behave similar to the pure Ag clusters and the transition is observed around 373 K. We see that progression bands are disappearing at 398 K as in the case of Ag clusters. It appears that the melting transition is reversible up to 448 K as is evidenced from spectrum h, which shows the data after cooling back from 448 K. The C–H stretching frequency came back to its original position.

As temperature increases, the factor group splitting is not seen; it appears that the two bands become almost identical and overlap and the doublets are not resolved. It has been reported that when monoclinic n-paraffins are heated above a certain temperature, they change slowly to an orthorhombic form and at a certain higher temperature they undergo a first-order transition to a hexagonal form, before melting. After the transition temperature, the split-peak structure disappeared.[23] This shows that the monolayer on the AuAg$_{0.5}$ cluster is behaving like n-paraffins.

Summary and Conclusions

The X-ray diffraction data of alloy cluster solids show low-angle peaks corresponding to larger unit cells suggesting the formation of CS-MPACs. For the entire composition range studied, only single cubic unit cells are obtained. The compositions differ substantially from that of the metal ion mixture used originally for the synthesis. To make a comparison, the crystalline solid of a mixture of Au and Ag clusters made by separate reduction was also investigated which again yielded a single cubic unit cell. These solids are distinctly different from the crystalline solids of ODT-protected Ag clusters (AgODT), in structural and spectroscopic features. In Au-rich compositions of the alloys, there are strong interactions between the alkyl chains yielding factor group splitting of some of the bands. The monolayer coverage is found to increase with increasing Ag composition.

In conclusion, the study shows that alloy cluster superstructures are distinctly different solids, showing characteristic structural, spectroscopic, thermal and calorimetric properties compared to the solids of mono-metallic clusters. However, the alkyl chain assembly in the two systems is similar, which in turn resemble that of crystalline alkanes. However, repeated heating/cooling cycles increase the alkyl chain order and reduce the fraction of the superstructure. This suggests that the alkyl chain assembly in the superstructure is less ordered than in crystalline alkanes and planar monolayers. Removal of defects results in the emergence of factor group-split peaks. Thus, the interactions leading to factor group splitting arise between the chains assembled on a single cluster.

Diverse properties should be possible with variation in the composition of the clusters. The fact that Au and Ag can be alloyed with a number of metals, several variations of crystalline alloy cluster solids can be prepared. In all of these cases, ordered superlattices of the clusters will make solid-state investigations more meaningful. We are currently extending this chemistry to chemically similar metal systems.